JOURNAL OF MATERIALS SCIENCE **35** (2000) 1397–1404

Powder prepared by spray pyrolysis as an electrode material for solid oxide fuel cells

R. MARIC, T. FUKUI, S. OHARA
Japan Fine Ceramics Center, 2-4-1, Mutsuno, Atsuta-ku, Nagoya 456-8587, Japan
E-mail: Maric@jfcc.or.jp

H. YOSHIDA, M. NISHIMURA, T. INAGAKI
Technical Research Center, The Kansai Electric Power Company, Inc, 11-20 Nakoji 3-chome Amagasaki, Hyogo 661-0974, Japan

K. MIURA
Kanden Kako Co. Ltd., Showa-dori, Amagasaki, Hyogo 606-0881, Japan

A variety of spray pyrolysis (SP) techniques have been developed to directly produce ceramic powders from solutions. Examples that are discussed include the following powders: $(La_{0.8}Sr_{0.2})_{0.9}MnO_3$-YSZ (La(Sr)$MnO_3$-YSZ), $La_{0.6}Sr_{0.4}CoO_3$ (La(Sr)CoO_3), $(CeO_2)_{0.8}(SmO_{1.5})_{0.2}$-NiO (SDC-NiO) and $La_{0.9}Sr_{0.1}Ga_{0.8}Mg_{0.2}O_3$-NiO (LSGM-NiO). For all these powders, spherical, non-agglomerated, submicrometer particles were obtained from aqueous solution of metal salts into a furnace using an ultrasonic atomizer at 1.7 MHz. After SP some of the particles exhibit a hollow-shell morphology. Subsequent calcination at 1000°C yielded crystalline particles. The electrical performance of Ni-SDC/LSGM/La(Sr)CoO_3 fuel cells operating at 800°C, prepared from the powders obtained by SP, is reported. © *2000 Kluwer Academic Publishers*

1. Introduction

Spray pyrolysis is an advanced method which enables spherical powder to be prepared through the pyrolysis or hydrolysis reaction of an atomized droplet containing the precursor [1–3]. Typically, solutions containing ionic or molecular solutes are converted to powders through the following steps [4, 5]: (1) solution droplet formation using an aerosol generator, (2) solvent evaporation and solute precipitation near the reactor entrance, (3) decomposition of the solute to the ceramic powder at higher temperatures in the main part of the reactor, and (4) sintering. To date most reactor systems have been designed such that the thermolysis and sintering processes overlap. Overlap of these processes in a single droplet could significantly affect densification of the particles. Therefore, a special separate reactor has been recently used in Japan Fine Ceramics Center (JFCC), see Fig. 1, to obtain maximum control of the evaporation, thermolysis and sintering processes and because of this the time temperature conditions are significantly different. In this manner, the advantages of starting with a solution are complemented by providing unique control over the thermolysis and sintering stages of inorganic particle formation. Most previous studies [6–10] emphasized the compositional flexibility for synthesizing ceramic powders but there have been few attempts to understand or model the processes and factors that affect the production of particles with controlled size and morphology. Recent achievements in the field of the synthesis of powders by powder processing have shown that chemical and physical properties of ceramic materials are highly dependent on the morphology and chemical composition of the starting powder [11–13]. Therefore, various properties of ceramic materials are expected to be improved by controlling the morphology and composition of the starting powder.

In order to make highly efficient solid oxide fuel cells (SOFCs) we have been applying nanostructured, composite powders obtained by SP as electrode materials [14–17]. Our preliminary studies on the electrodes prepared from SP obtained powders showed the importance of microstructure control to obtain good performing electrodes for SOFCs. The unit cell of SOFCs consists of a three-layer structure: anode, electrolyte, and cathode. The application of composite powder as electrode materials results in enlargement of the effective reaction zone to include the entire particle surface beyond the boundary zone of the physical contact points to be the reaction area. The cathode, which is maintained in an oxidizing atmosphere, is usually an oxide doped for high electrical conductivity, such as strontium doped lanthanum manganite. The anode, on the other hand, is maintained in a reducing atmosphere and is usually a cermet such as nickel-zirconia. In order to improve efficiency, the microstructure of each electrode of the SOFC must be optimized.

The goal of this study was to synthesize composite powder with controlled morphology by the spray pyrolysis method in order to obtain high-performance

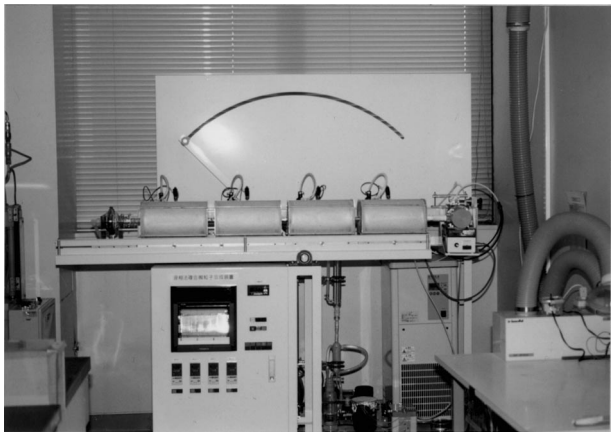

Figure 1 Spray pyrolysis equipment.

anodes and cathodes. The influence of microstructure on electrical performance of the Ni-SDC/LSGM/ $La(Sr)CoO_3$ fuel cell has been investigated.

2. Experimental procedure

2.1. Materials

The powders included in the present investigation were $(La_{0.8}Sr_{0.2})_{0.9}MnO_3$-YSZ, $La_{0.6}Sr_{0.4}CoO_3$, $(CeO_2)_{0.8}(SmO_{1.5})_{0.2}$-NiO (SDC-NiO) and $La_{0.9}Sr_{0.1}Ga_{0.8}Mg_{0.2}O_3$-NiO (LSGM-NiO).

2.1.1. $(La_{0.8}Sr_{0.2})_{0.9}MnO_3$-YSZ and $La_{0.6}Sr_{0.4}CoO_3$

$La(Sr)MnO_3$-YSZ and $LaSrCoO_3$ have been used as cathode materials for SOFC. $La(Sr)MnO_3$ and $La(Sr)CoO_3$ have perovskite-like structures, with characteristic lattice distortion and multiple unite cells which are a result of partial covalent bonding. $La(Sr)MnO_3$-YSZ composite particles were prepared from YSZ sol (8-mol% yttria-stabilized zirconia sol, Nissan chemical Product Ltd.), (La, Sr) MnO_3 derivatives by the SP technique. La_2O_3, $SrCO_3$, and MnO_2 were dissolved together in an aqueous nitrate and hydrogen peroxide, and pure water. YSZ sol solution was added to the solution. To obtain A site defect type $(La_{0.8}Sr_{0.2})_{0.9}MnO_3$, the molar ratio of La, Sr, and Mn in the solution (0.1 mol/L) was La : Sr : Mn = 0.72 : 0.18 : 1. $(La_{0.8}Sr_{0.2})_{0.9}MnO_3$: YSZ = 50 : 50 (mol%) was applied to the initial composition. Similarly, La_2O_3, $SrCO_3$, and Co_2O_3 were used to make $La_{0.6}Sr_{0.4}CoO_3$.

2.1.2. $(CeO_2)_{0.8}(SmO_{1.5})_{0.2}$-NiO (SDC-NiO) and $La_{0.9}Sr_{0.1}Ga_{0.8}Mg_{0.2}O_3$-NiO (LSGM-NiO)

Mixed conducting oxide particles, samaria-doped ceria (SDC) and oxide ion conductor particles, doped lanthanum gallate, were employed as the anode material utilizing a highly dispersed noble metal catalyst Ni. For one cell, ceria is partially reduced in the reducing atmosphere at the anode side of the fuel cell and becomes a mixed conductor to both electrons and oxide ions. The use of a mixed conducting oxide anode results in an enlarged electrochemical reaction zone beyond the physical triple-phase boundary. $(CeO2)_{0.8}(SmO_{1.5})_{0.2}$(SDC)-NiO composite particles were obtained from solution, which was prepared from $Ce(NO_3)_3{\cdot}H_2O$, Sm_2O_3 and $Ni(CH_3COO)_2{\cdot}4H_2O$ raw materials. The volume ratio of the SDC to Ni

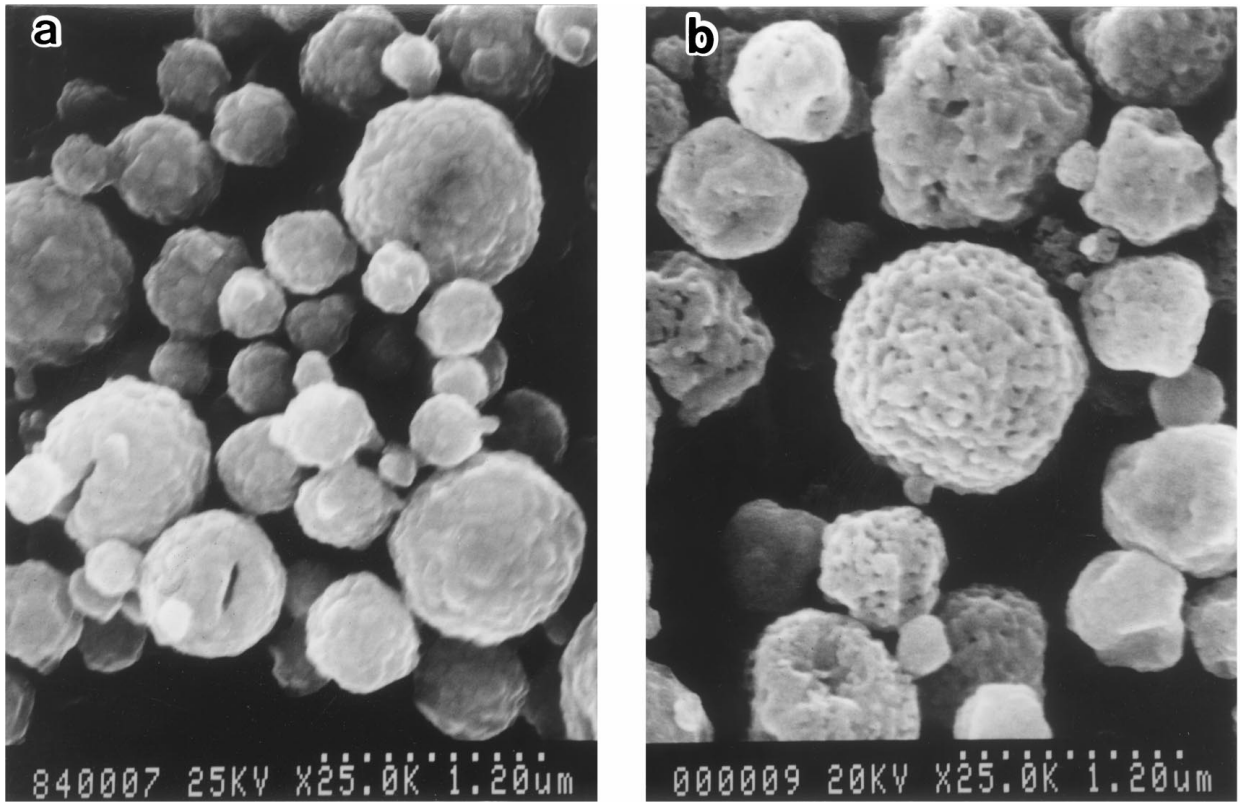

Figure 2 SEM micrographs of a) $La_{0.8}Sr_{0.2}MnO_3$-YSZ, and b) $La_{0.6}Sr_{0.4}CoO_3$ synthesized powder after SP.

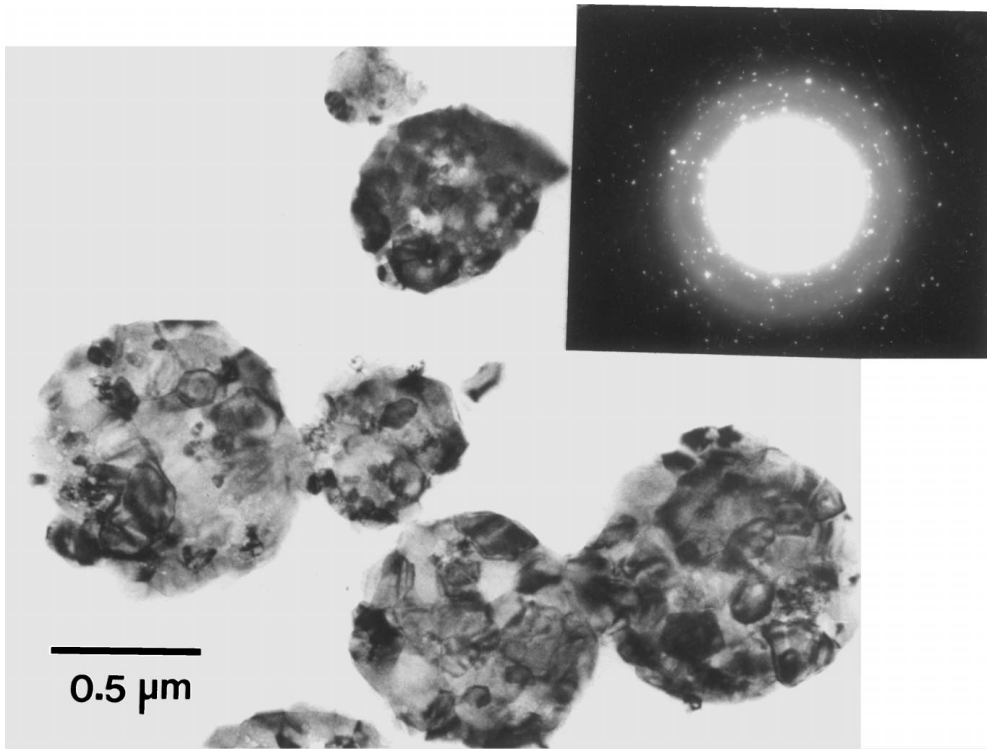

Figure 3 TEM bright-field image and diffraction pattern of $La_{0.8}Sr_{0.2}MnO_3$-YSZ composite powder prepared by SP.

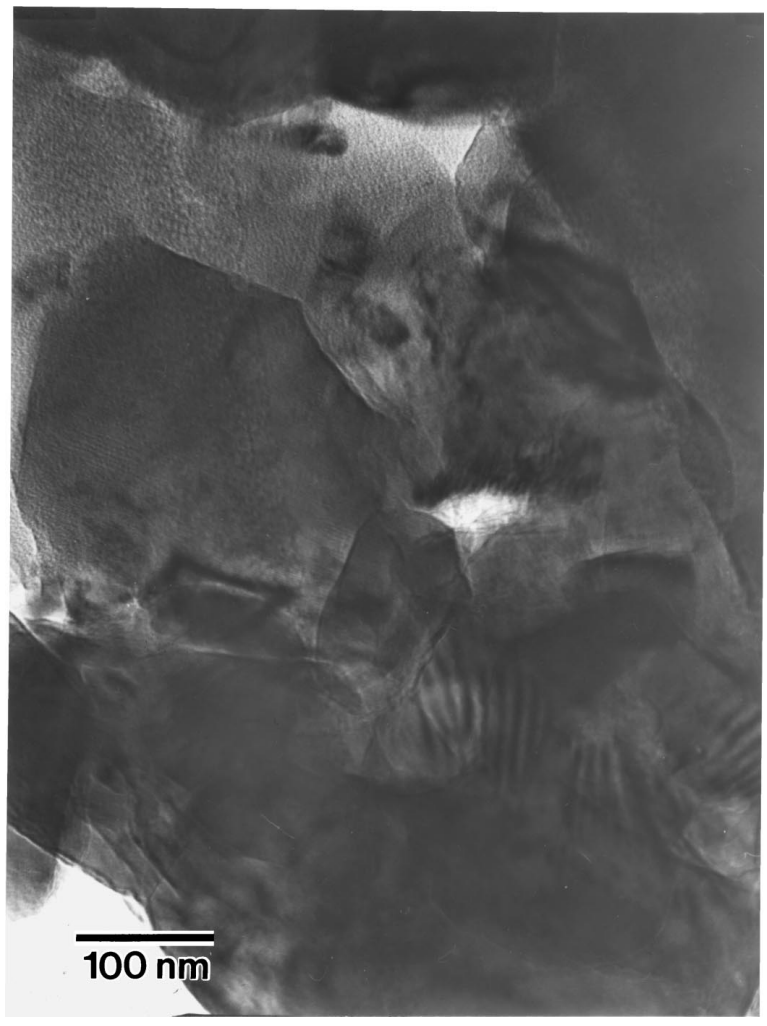

Figure 4 TEM bright-field image of $La_{0.6}Sr_{0.4}CoO_3$ powder after SP.

was 50 : 50. $La_{0.9}Sr_{0.1}Ga_{0.8}Mg_{0.2}O_3$-NiO composite particles were prepared from La_2O_3, $SrCO_3$, and $Mg(CH_3COO)_2{\cdot}4H_2O$ raw materials and were dissolved together in $Ni(CH_3COO)_2{\cdot}4H_2O$. The volume ratio of the LSGM to Ni was 50 : 50. These initial solutions were atomized with an ultrasonic vibrator operated at 1.7 MHz. Droplets were transported to a reaction furnace using air as a carrier gas with a fixed flow rate of 3 L/min. The reactor consisted of four independent heating zones. The temperatures of each heating zone—zone 1, zone 2, zone 3, and zone 4—were set at 200, 400, 800, and 1000°C, respectively. The particles from the furnace outlet were collected using an organic filter. After SP the powder was calcinated at temperature of 1000°C for several hours.

2.2. Powder characterization

X-ray diffraction (XRD) analysis (Phillips Diffractometer PV 9900) was used to identify the phases of the as-synthesized and calcinated powders. The morphology and microstructure of the composite powder were

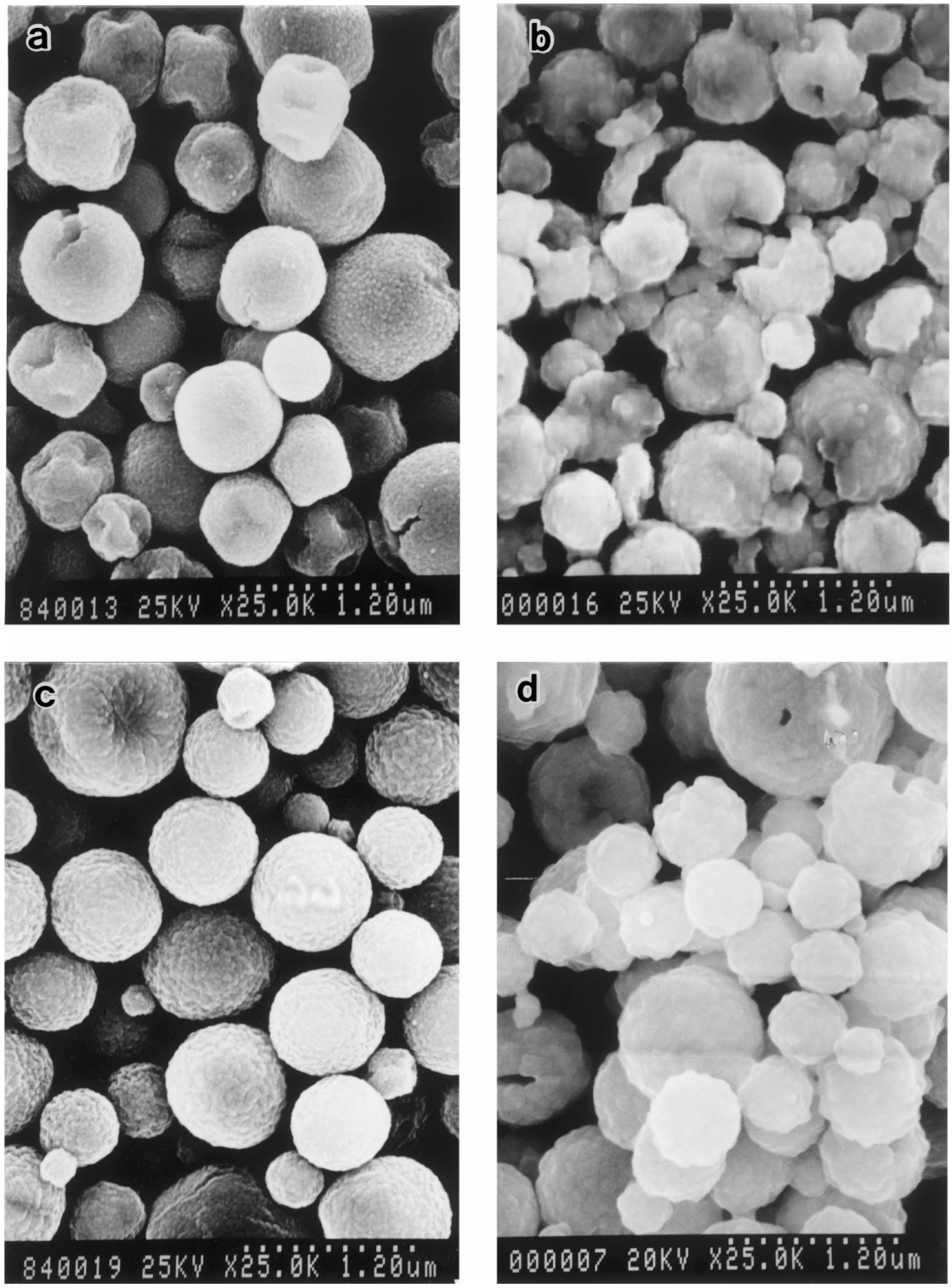

Figure 5 SEM micrographs of a) $(CeO_2)_{0.8}(SmO_{1.5})_{0.2}$-NiO (SDC-NiO) after SP, b) SDC-NiO after calcination, c) $La_{0.9}Sr_{0.1}Ga_{0.8}Mg_{0.2}O_3$-NiO (LSGM-NiO) after SP and d) LSGM-NiO after calcination.

studied using scanning electron microscopy (SEM, Hitachi, S-800) with an energy dispersive analysis of X-ray (EDAX; Philips, PV9900). TEM (JEOL JEM-200) was employed to investigate the crystallite size distribution and using dark-field images we were able to measure the size of the crystals.

2.3. Electrochemical characteristics

For the electrochemical characterization of a SOFC, the current-interruption technique was used. The anode and cathode layers were deposited by a screen printing technique onto a commercial dense electrolyte disk. The preparation of the cells and operating conditions are as described in our previous studies [14, 15, 18].

3. Results and discussion

3.1. Cathode powder

As shown in Fig. 2 a spherical particle morphology has been obtained by SP processing of cathode powder. It is clear from this figure that the shape of the particles is equiaxial and uniform. For La(Sr)MnO_3-YSZ and La(Sr)CoO_3 each particle seems to be an aggregate of small, individual crystallites about 100 nm in diameter. TEM observation of the powder was carried out in order to evaluate the microstructure of the particles in detail. Fig. 3 shows a TEM photograph of La(Sr)MnO_3-YSZ particles embedded in an epoxy resin, prepared by ion beam milling. It is obvious that dense particles consist of fine crystallites smaller than 100 nm. TEM-EDS analysis showed that the fine crystallites contained either the elements La-Sr-Mn-O or Y-ZrO [3]. The particle morphology of La(Sr)CoO_3 is shown in Fig. 4. It is seen in Fig. 4 that the particle consists of many crystallites about 100–200 nm in diameter. The morphology of the composite powder can be controlled by the controlling the synthesis conditions of SP. As presented by Messing *et al.* [19] there are a number of possibilities for synthesizing multicomponent and composite particles with a unique range of microstructure characteristics. The morphology of the particles can be predicted from model calculations of the solute concentration gradient and a simple criterion for solid particle formation. High initial solute concentration inside the droplet is suitable for the volume precipitation which leads to solid particle formation. If the initial concentration is lower than the equilibrium saturation, surface precipitation should occur, and surface precipitation seems to be the cause of hollow particle formation.

3.2. Anode powder

For SDC-NiO anode powders, particles formed by SP are composed of crystallites substantially less than 100 nm in diameter, Fig. 5a. After calcination of SDC-NiO powder the particle morphology remains spherical and particles are composed of many crystallites about 100 nm in diameter, Fig. 5b. To confirm the size of the crystallites X-ray diffraction pattern of the SDC-NiO powder obtained after SP and calcination has been used,

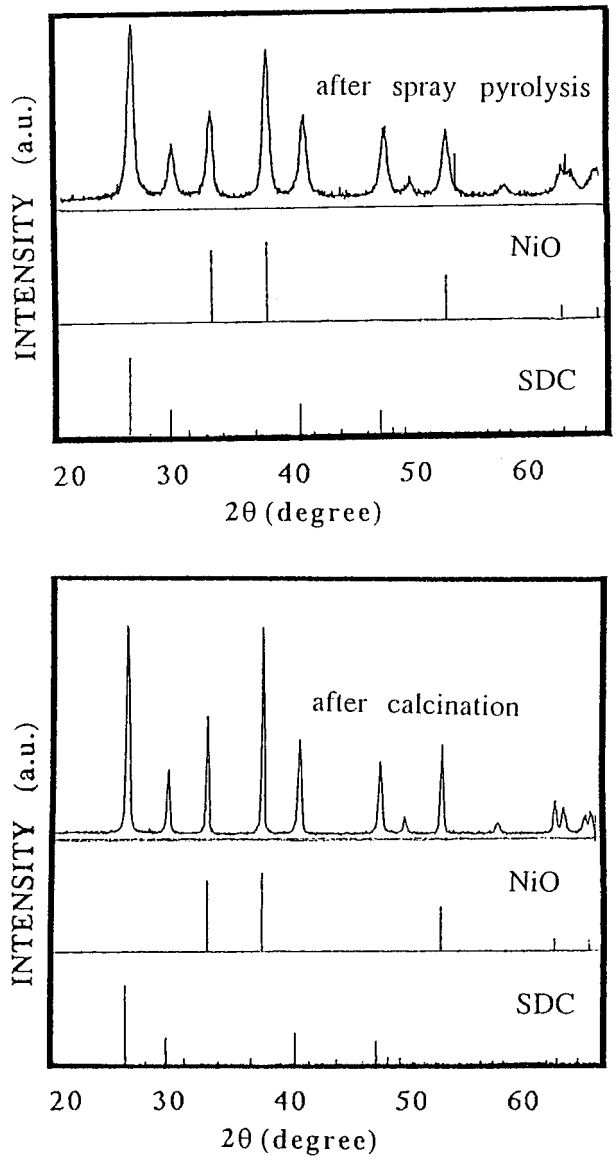

Figure 6 X-ray diffraction patterns for SDC-NiO powders after a) SP, and b) after calcination.

Fig. 6. The crystallite size of the powder obtained after SP has been calculated from an X-ray diffraction peak broadening by the Scherror formula [20] and for SDC and NiO crystallites were 15 and 20 nm, respectively. During calcination the crystallite sizes of both components increased and for SDC and NiO after calcination attained values were about 85 and 100 nm, respectively.

SP prepared LSGM-NiO powder consists of highly spherical powder particles which have a wide range of diameters, Fig. 5c. The minimum to maximum particle size observed in Fig. 5c is 0.2–1 μm. Each spherical powder particle appears to consist of an agglomeration of smaller crystallites. This is illustrated more clearly by observing the powders using transmission electron microscopy; the transmission electron micrograph of the LSGM-NiO particles shown in Fig. 7a confirms that particles have been almost amorphous after SP. During calcination crystallite formation occurred and particles were composed of many crystallite as shown in Fig. 5d. The TEM micrographs in Fig. 7b show that calcination of this powder at 1000°C brings a crystalline structure and if the powder produced by SP consisted of hollow

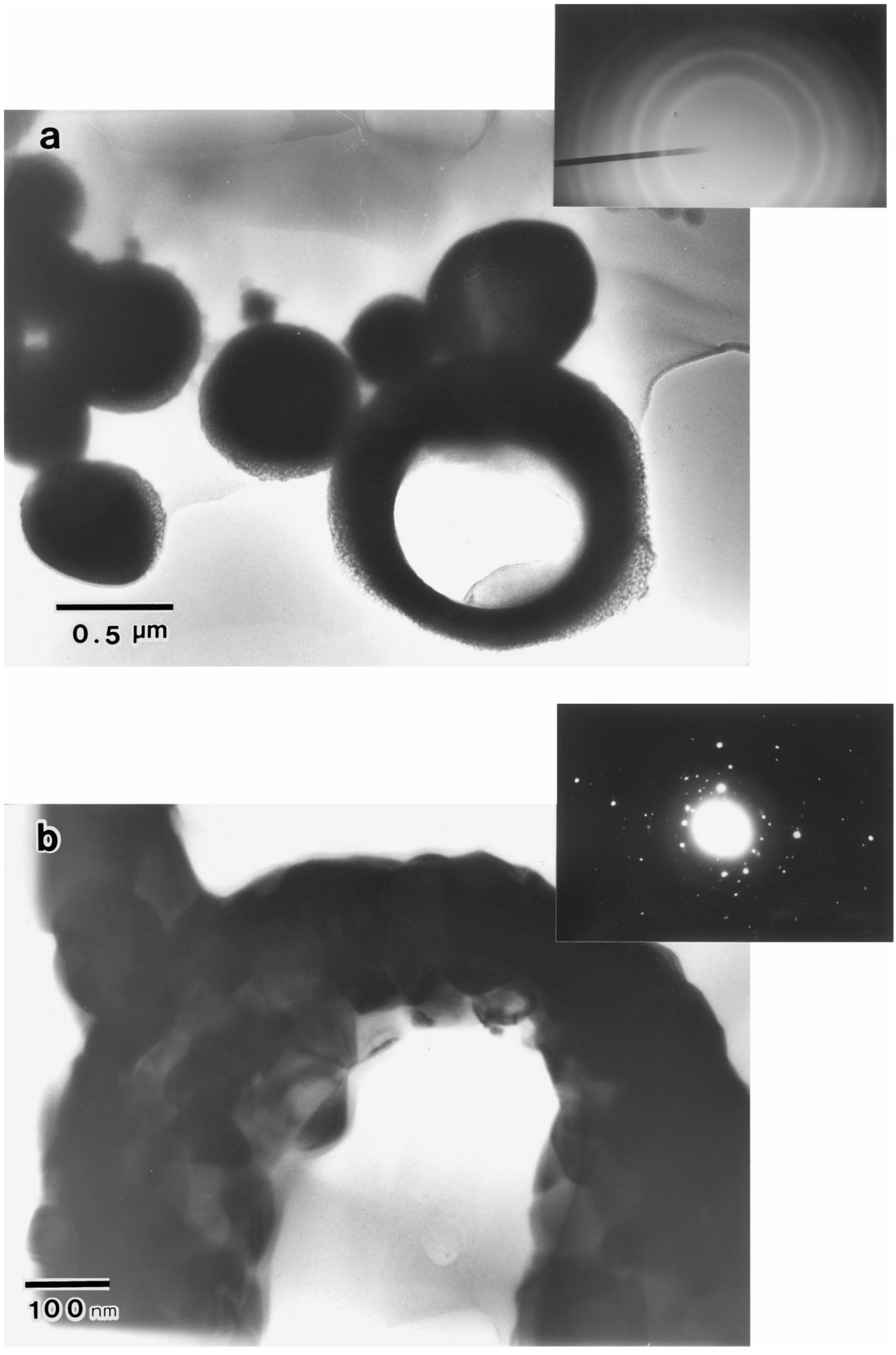

Figure 7 The bright field images and the corresponding diffraction patterns of $La_{0.9}Sr_{0.1}Ga_{0.8}Mg_{0.2}O_3$-NiO (LSGM-NiO) powder a) after SP, and b) after calcination at 1000°C for 2 h.

spheres that hollow spheres will also remain during calcination. As shown in Fig. 6b the particle consists of a uniform mixture of 90 nm NiO and 75 nm LSGM crystallites. One of our attempts is to explain marphology of the powder formed during SP processing. Based on precipitation theory, Leong [21] reported that the degree of supersaturation influences the size and number of the crystals formed in the droplet. Solutes with a high degree of supersaturation tend to form a large number of nano-meter sized crystallites, and, thus, the shape of the particles is spherical. Conversely, when the degree of supersaturation is low, the nucleation rate is small relative to the growth rate, and therefore, only a few large crystals and in some cases, even single crystals are formed. The size and number of the crystals determine the size and size distribution of the pores. In some big particles of LSGM-NiO a hollow structure has been found, Fig. 7a. The reason for this morphology can be attributed to the fast nucleation rate of the precursor from the outer part of the droplet or the difficulty in degassing the residual gas.

4. Application of SP powders as electrodes in SOFC

The current-interruption technique has been used to study the effect of the microstructure, grain size and porosity on the electrical properties of SOFC electrodes [15, 18, 22].

The maximum power density of a La(Sr)MnO_3-YSZ/YSZ/Ni-YSZ cell operating at 1000°C was over 380 mW/cm^2 and the electrical performance of this cell has been discussed in more detail in a previous study [15]. Therefore, only present results obtained for the Ni-SDC/LSGM/LSCo cell operating at 800°C are discussed.

Application of SDC-NiO, and LSGM-NiO as anode materials in SOFC significantly lowered the operation temperature of the cell due to their high oxide ionic conductivity. Since polarization characteristics of the anode depend strongly on powder microstructure, good electrical contact of the consisting particles (Ni to Ni, Ni to SDC, and SDC to SDC) is important. Fig. 8 shows i-V and i-P curves obtained with a La(Sr)CoO_3 cathode and Ni-SDC cermet anode. The maximum power density of the cell is about 425 mW/cm^2, which is 95% of the theoretical value 447 mW/cm^2 (electrolyte thickness: 500 μm, electrolyte conductivity: 0.075 S/cm, and OCV: 1.09 V). This high performance seems to be due to the microstructure, in which Ni particles form a skeleton with well-connected SDC particles finely distributed over the Ni particle surfaces [18], and the cathode microstructure consisted of small and well-connected LSCo particles [22]. In general, the immigration of feed gas and product depends on the electrode morphology, and the exchange of charge depends on the length of the three phase boundary and the activity of the electrode materials. Therefore, the overall efficiency of SOFC is greatly controlled by the morphology of the electrodes.

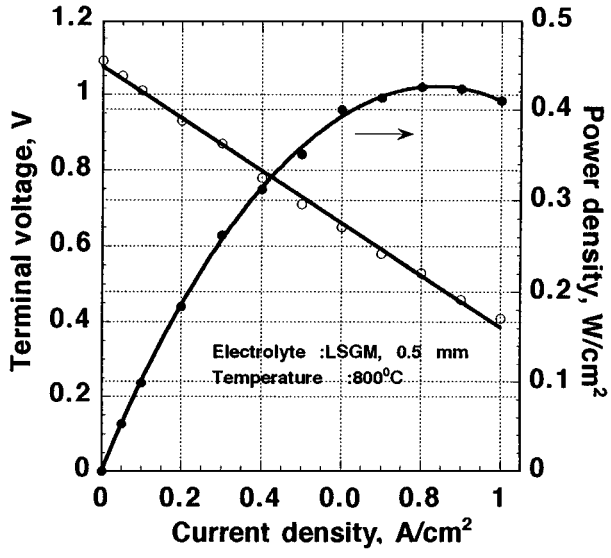

Figure 8 Single fuel cell performance Ni-SDC/LSGM/LSCo at 800°C.

5. Conclusions

We have shown that the spray pyrolysis technique can be successfully applied to the fabrication of composite powder. The mean particle size of $La_{0.8}Sr_{0.2}MnO_3$-YSZ, $La_{0.6}Sr_{0.4}CoO_3$, $(CeO_2)_{0.8}(SmO_{1.5})_{0.2}$-NiO (SDC-Ni) and $La_{0.9}Sr_{0.1}Ga_{0.8}Mg_{0.2}O_3$-NiO (LSGM-NiO) powders was about 1 μm. As confirmed by X-ray, elemental analysis, SEM, and TEM the particles consist of many crystallites, and for La(Sr)MnO_3-YSZ and La(Sr)CoO_3 the mean crystallite size was about 100 nm. SDC-NiO consisted of many fine crystallites of SDC and NiO about 20 nm in diameter. In the case of LSGM-NiO an amorphous structure was formed but after calcination it became crystalline. Using composite powder obtained by SP as electrode materials SOFC, we demonstrated that the high performance of two types of SOFCs, performance is strongly influenced by the electrodes microstructure. The maximum power density of Ni-YSZ/YSZ/La(Sr)MnO3-YSZ operating at 1000°C, and Ni-SDC/LSGM/LSCo operating at 800°C cells were 380 and 425 mW/cm^2, respectively. These improved performances were attributed to the development of electrodes with optimized microstructures from fine powders prepared by SP.

References

1. Y. KANO and T. SUZUKI, *J. Mater. Sci.* **23** (1988) 3067.
2. N. TOHKE, M. TATSUMISAGO and T. MINAMI, *J. Am. Ceram. Soc.* **74** (1991) 2117.
3. T. FUKUI, T. OBUCHI, Y. IKUHARA, S. OHARA and K. KODERA, *ibid.* **80** (1997) 261.
4. C. ZHANG, G. L. MESSING and M. BORDEN, *ibid.* **73** (1990) 61.
5. T. T. KODAS, *Angew. Chem. Int.* Ed. Engl. **28** (1989) 794.
6. D. M. ROY and S. O. OYEFESOBI, *J. Am. Ceram. Soc.* **60** (1977) 178.
7. E. FOA, C. FRIEDMAN, J. BIRNBAUM, Y. SCHACTER and M. KONIGSBUCH, *Isr. J. Technol.* **10** (1972) 433.
8. D. M. ROY and S. O. OYEFESOBI, *J. Am. Ceram. Soc.* **60** (1977) 178.
9. T. P. O'HOLLERAN, R. R. NEORGAONKAR, D. M. ROY and R. ROY, *Am. Ceram. Soc. Bull.* **57** (1978) 459.

10. O. SAKURAI, M. MIYAUCHI, N. MIZUTANI and M. KATO, *J. Ceram. Soc. Jpn.* **97** (1989) 398.
11. M. WATANABE, T. SAEGUSAN and P. STONEHART, *J. Electroanal. Chem.* **271** (1989) 213.
12. D. W. DEES, *J. Electrochem. Soc.* **134** (1987) 2141.
13. T. H. ESTELL and S. N. FLENGAS, *ibid.* **118** (1971) 1890.
14. S. OHARA, T. FUKUI, K. MUKAI, K. KODERA and Y. KUBO, in "Proceedings of the 5th International Symposium on Solid Oxide Fuel Cells," edited by U. Stimming, S. C. Singhal, H. Tagawa and W. Lehnert, The Electrochemical Society Proceedings Series, (Pennington, NJ, 1997) p. 815.
15. T. FUKUI, S. OHARA and K. MUKAI, *Electrochem. and Solid-State Letter* **1** (1998) 120.
16. S. OHARA, K. MUKAI and T. FUKUI, in Proceeding of the 1998 Fuel Cell Seminar Abstracts, Palm Springs, 1998, p. 128.
17. R. MARIC, T. FUKUI, S. OHARA and Y. KUBO, in "Processing and Properties of Advanced Engineering Materials," edited by T. Kobayashi, M. Umemoto and M. Morinaga, (ISAEM-97, Toyohashi, 1997), p. 319.
18. R. MARIC, S. OHARA, T. FUKUI, T. INAGAKI and J. FUJITA, *Electrochem. and Solid-State Letters*. **1** (1998) 201.
19. D. W. SPRONSON and G. L. MESSING, in "Ceramic Powder Science," edited by G. L. Messing, K. S. Mazdiyasni, J. W. McCauley and R. A. Haber (American Ceramic Society, Westerville, OH, 1987).
20. R. MARIC, S. OHARA, T. FUKUI and Y. KUBO, *J. Am. Ceram. Soc.*, to be published.
21. K. H. LEONG, *J. Aerosol. Sci.* **18** (1987) 527.
22. R. MARIC, S. OHARA, T. FUKUI, H. YOSHIDA, M. NISHIMURA, T. INAGAKI and K. MIURA, *J . Electrochem. Soc.*, to be published.

Received 2 February
and accepted 11 August 1999